

## Structural and vibrational properties of Si clathrates in a generalized tight-binding molecular-dynamics scheme

Madhu Menon,\* Ernst Richter, and K. R. Subbaswamy

*Department of Physics and Astronomy, University of Kentucky, Lexington, Kentucky 40506*

(Received 12 June 1997)

The structural and vibrational properties of Si in two fourfold coordinated crystalline structures (clathrates) are studied and compared with those in the diamond structure using a generalized tight-binding molecular-dynamics scheme. The vibrational spectra reported for both clathrates are obtained using quantum methods and contain many interesting features, the most striking being the presence of a gap. Additionally, theoretical Raman spectra for these clathrates are also presented. [S0163-1829(97)08741-9]

### I. INTRODUCTION

The possibility of altering semiconductor band gaps has generated considerable interest recently. This is because band gap engineering enables control over the wavelength of light emitted, making it possible to generate photoluminescence in the visible region with important technological implications. A number of pathways towards this end have been proposed. They include making Si in ‘‘porous’’ form,<sup>1,2</sup> which causes the band gap to be increased. Although confinement effect has been suggested as a possible cause for this increase,<sup>3</sup> the full mechanism of the band gap increase is not yet fully understood.<sup>4</sup> Formation of alloys with Si as one of the components provides an alternate route towards changing the band gap. The widely studied  $\text{Si}_{1-x}\text{Ge}_x$ , however, has smaller band gap when compared to that of diamond Si.<sup>5</sup>

It was found that a whole new class of materials called clathrates can be generated by altering the bond angles from their ideal tetrahedral value in the diamond structure.<sup>6-10</sup> The clathrates form local minima of the total energy and some of them are only slightly less stable than the diamond phase. The silicon-clathrate compounds are not attacked even by strong acids except for HF. Importantly, the band gaps of these structures are substantially larger than that of Si in the diamond structure and well into the visible region. It is worth noting that the high pressure phases of bulk Si such as  $\beta$ -Sn, on the other hand, are metallic with no gap. The clathrate structures are relatively open, allowing for endohedral impurity atoms.

The experimental synthesis of clathrates involves two steps.<sup>11</sup> The first step involves reacting of Si powder or pieces of Si wafer with alkali metal (*A*) at 580 °C for few hours inside an airtight stainless steel bomb sealed in a quartz tube under vacuum of 10–3 Torr. This reaction yields alkali metal silicide *ASi*, together with excess alkali metal. In the second step, the *ASi/A* mixture is heated under a dynamic vacuum for about 30 hours at temperatures 300–450 °C, to form Si clathrate phase.<sup>12</sup>

In this work we examine the structural and vibrational properties of the lowest energy clathrates;<sup>6</sup> specifically a clathrate structure containing 34 atoms in a face-centered cubic (fcc) unit cell and another structure containing 46 at-

oms in a simple-cubic (sc) unit cell, using a generalized tight-binding molecular-dynamics (GTBMD) scheme. We denote these clathrate structures by Clath34 and Clath46, respectively. Figure 1 shows drawings of these structures. In particular, we report on the full (symmetry unrestricted) relaxation of the structures within a constant pressure molecular-dynamics simulation. The expected Raman spectra from these crystals are also calculated within a bond polarizability model.

Although molecular-dynamics simulations have been used by other groups in earlier works on these clathrates, the lattice constant was taken to be fixed during the simulations (constant volume). Also, no first principles methods have been used to date in the investigation of vibrational properties of these systems.<sup>7,8</sup> In the present work, incorporation of the constant pressure ensemble into the GTBMD allows for simultaneous relaxation of the lattice and basis degrees of freedom. This is crucial in testing stability and obtaining vibrational frequencies as a true local minimum can be achieved within the model.

### II. THEORETICAL SCHEME

The theoretical method used in the present work is the generalized tight-binding molecular-dynamics<sup>13-15</sup> (GTBMD) scheme of Menon and Subbaswamy that allows for full relaxation of covalent systems with no symmetry constraints. The GTBMD method differs from the conventional tight-binding methods in that explicit use of nonorthogonal-

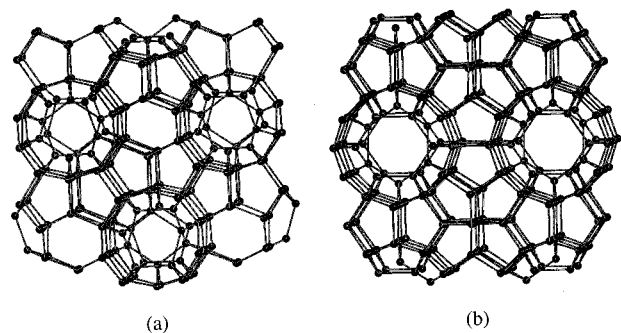


FIG. 1. (a) The Clath(34) structure and (b) the Clath(46) structure.

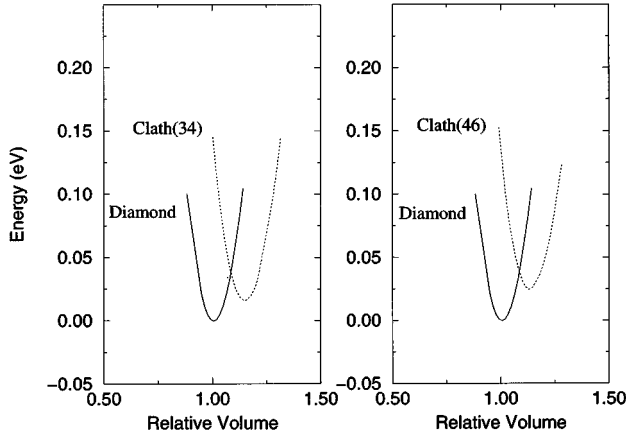


FIG. 2. Energy per atom in eV as a function of the relative volume per atom for the diamond structure, Clath(34) and Clath(46).

ity of the basis is made in the formalism. This allows for proper accounting of the local coordination information in the electronic structure Hamiltonian, resulting in excellent transferability for structural and vibrational properties of Si from dimer through bulk with only a minimal number of adjustable parameters. The equilibrium bond lengths for the dimer and bulk diamond structure are obtained to be 2.22 and 2.36 Å, respectively.<sup>15</sup> This compares very favorably with the experimental values of 2.24 Å and 2.35 Å, respectively.<sup>25</sup> Application of GTBMD to obtain equilibrium geometries for small silicon clusters<sup>13–15</sup> has yielded good agreement with *ab initio* results.<sup>16</sup> When applied to the bulk phases of Si, GTBMD has reproduced binding energy differences between the high-pressure metallic phases and the diamond phase in excellent agreement with the schemes based on the local density approximation (LDA).<sup>15</sup> Furthermore, the GTBMD scheme predicts clathrate phases to be higher in energy when compared with the diamond phase (see Fig. 2).<sup>14,15</sup> This is important when one considers the fact that most conventional orthogonal schemes, while giving good results for the higher density phases of Si ( $\beta$ -tin, simple cubic, and fcc), predict the clathrate phase to be the ground state, in disagreement with LDA results and experiment.<sup>8</sup> The correct ordering of the cohesive energies of diamond and clathrate structures, thus, gives us confidence in the interpretation of the results obtained using the GTBMD scheme. Also, as shown in the next section, the results for the structural parameters are in excellent agreement with LDA based results for these clathrates. GTBMD has also been found reliable in obtaining good agreement with experimental and local density approximation (LDA) results for the

structural and vibrational properties of fullerenes and nanotubes.<sup>17</sup>

For the treatment of clathrate structures, a constant pressure ensemble method was incorporated into the GTBMD scheme to allow for realistic lattice relaxation. This is necessitated by the fact that these structures contain a large number of atoms in the unit cell, making the structure dependent on the choice of the lattice parameters. The constant pressure MD method was first introduced by Andersen<sup>18</sup> and subsequently extended by Parrinello and Rahman.<sup>19</sup> Its usefulness in applications to structural changes in the solid state phases has been amply demonstrated in recent works.<sup>19–22</sup>

### III. RESULTS

#### A. Structural properties

In this section we present our results for clathrates obtained using the GTBMD scheme. For Clath34 we consider a face-centered cubic (fcc) lattice with a 34 atom basis. The minimum energy configuration is obtained by a symmetry unconstrained molecular-dynamics relaxation with a simultaneous symmetry unrestricted relaxation for the lattice parameters starting with an ideal  $Fd\bar{3}m$  geometry. We use a uniform grid of 8  $k$  points in the supercell in computing forces. Convergence was checked by increasing  $k$  points. The fully relaxed lattice maintained its  $Fd\bar{3}m$  symmetry with a cohesive energy 0.03 eV/atom lower when compared with diamond and a lattice constant of  $a = 14.69$  Å. This is in very good agreement with the LDA based calculations that predict the lattice constant  $a$  to lie between 14.46 Å and 14.86 Å, depending on the choice of the basis (e.g., plane wave or local orbital).<sup>7</sup> Four distinct bond lengths were obtained for this structure ranging from 2.343 Å to 2.385 Å with an average bond length of 2.366 Å. This compares favorably with the experimentally determined bond length of 2.37 Å for this clathrate.<sup>7</sup> The volume per atom is found to be increased by 14% when compared to diamond. In Table I we summarize our structural results and compare with LDA results.

In Fig. 3, we show the electronic band structure for Clath34. The top of the valence band is almost flat when compared to the band structure for Si in diamond structure.

We obtain an increase in the band gap of 0.61 eV for Clath34 over that for Si in bulk diamond structure.<sup>23</sup> This value compares very favorably with the value obtained by the LDA based scheme which finds an increase of 0.7 eV.<sup>7</sup> This widening of the gap has important technological implications when one considers the fact that Clath34 differs from diamond structure in only the bond angles. We also find that

TABLE I. Structural properties of Si clathrates.  $V_0$  is the volume of the diamond structure at its minimum energy.  $a$  denotes the equilibrium lattice constant.

	Lattice	Average bond length	$V/V_0$	$a$ (Å)
Diamond	fcc	2.36 (2.35) <sup>a</sup>	1.000	5.45 (5.43) <sup>a</sup>
Clath(34)	fcc	2.366 (2.37) <sup>a</sup>	1.14 (1.17) <sup>b</sup>	14.69 (14.46–14.86) <sup>b</sup>
Clath(46)	sc	2.367	1.14 (1.17) <sup>b</sup>	10.20 (10.35) <sup>b</sup>

<sup>a</sup>Reference 25.

<sup>b</sup>Reference 7.

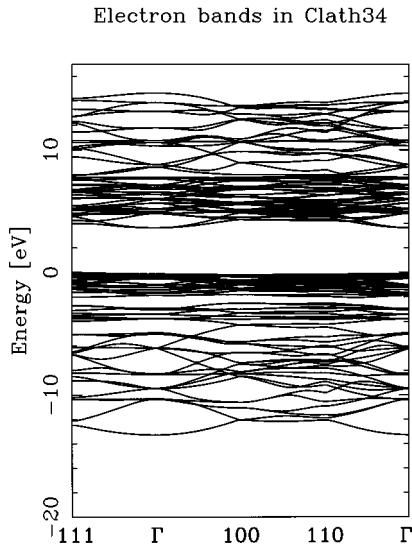


FIG. 3. Band structure of Clath34 obtained using the GTBMD scheme.

the valence band maximum has moved down in energy by 0.8 eV compared to the valence band maximum of Si in diamond structure.

For Clath46 we consider a simple cubic (sc) lattice with a 46 atom basis. The fully relaxed lattice maintained its ideal  $Pm3n$  symmetry with a cohesive energy 0.035 eV/atom lower when compared with the diamond structure and a lattice constant of  $a = 10.20$  Å. This is in very good agreement with the LDA based calculations that predict the lattice constant to be  $a = 10.35$  Å. Four distinct bond lengths were obtained for this structure ranging from 2.347 Å to 2.395 Å with an average bond length of 2.367 Å. The volume per atom is found to be increased by 14% when compared to Si in the diamond structure.

In Fig. 4, we show the electronic band structure for Clath46. The top of the valence band is, again, almost flat when compared to the band structure for Si in diamond

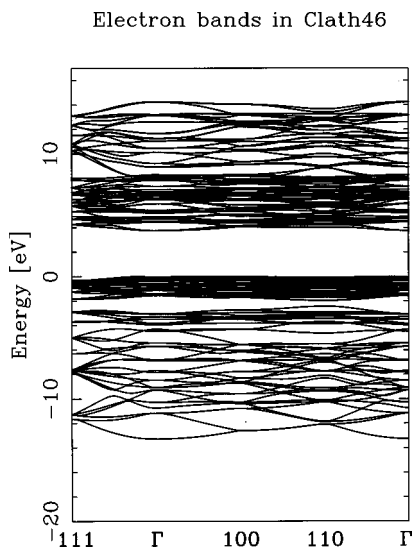


FIG. 4. Band structure of Clath46 obtained using the GTBMD scheme.

structure. We obtain an increase in the band gap of 0.65 eV for Clath46 over that for Si in bulk diamond structure. This value compares very favorably with the value obtained by the LDA based scheme which finds an increase of 0.7 eV.<sup>7</sup> For this clathrate we find that the valence band maximum has moved down in energy by 0.72 eV compared to the valence band maximum of Si in diamond structure. Both the valence band maximum and the conduction band minimum have moved up slightly when compared to Clath34. This trend is in qualitative agreement with the LDA based results reported in Ref. 7.

It is interesting to note that even though the top of the valence band for these clathrate structures moves down in energy compared to the diamond structure, the total energies for these structures are higher than in diamond. This is attributed to an increase in the strain energy on account of bond-bending which more than offsets the gain in electronic energy.

## B. Vibrational properties

In this section we present our results for the vibrational properties of clathrates obtained using the GTBMD scheme. The force constants for the evaluation of vibrational modes are obtained by explicitly calculating analytic second derivatives of the electronic structure Hamiltonian matrix elements.<sup>24</sup> This method, while providing better accuracy than numerical derivative schemes, greatly expedites the determination of vibrational modes for large size clusters. The phonon spectra were obtained by using precisely the same tight-binding parameters that were used in optimizing the geometries of the structures by molecular-dynamics relaxation.

The GTBMD scheme has been found to be reliable in obtaining good agreement with experiment for the diamond phase of bulk Si,<sup>15</sup> with the average deviation from the measured phonon values of only 8% and a maximum mode deviations of only up to about 13% from experiment.<sup>25</sup> It is worth noting that in determining the four adjustable parameters in the theory, primary consideration was given to reproducing only the structural properties of bulk and dimer, and no particular effort made to obtain accurate agreement for frequencies. Nevertheless, the degree of agreement obtained with experiment for frequencies using only four adjustable parameters is gratifying.

The clathrate structures provide an interesting contrast when compared to the diamond phase of Si in their vibrational properties. This is due to the fact that, even though clathrates have the same coordination as Si in the diamond phase, there are four distinct bond lengths when compared to only one for the diamond phase. Additionally, the deviation in the bond angles from their ideal tetrahedral value in the diamond structure also contributes to the differences in vibrational spectra.

Previous calculations of Si clathrates have relied on the use of force constant models using a Keating type potential energy expression and a preassigned (unoptimized) geometry.<sup>26</sup> The highly directional nature of the electronic distribution in these covalent materials makes transferability of classical potentials in different environments inadequate. Additionally, the search for true ground state must involve a simultaneous symmetry unrestricted optimization of both lat-

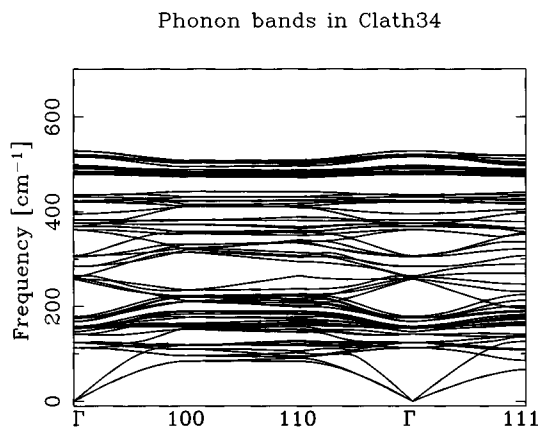


FIG. 5. Phonon dispersion curves for Clath34 obtained using the GTBMD scheme.

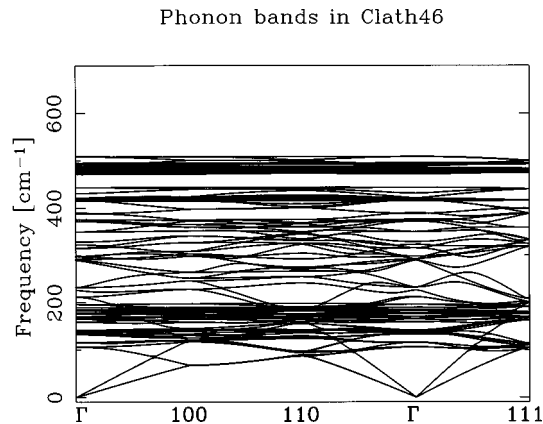


FIG. 6. Phonon dispersion curves for Clath46 obtained using the GTBMD scheme.

tice and basis vectors prior to obtaining frequency estimations. The present method, due to its quantum mechanical nature, provides a realistic treatment of differing structural environments with electronic degrees of freedom rearranged accordingly. Furthermore, the use of the constant pressure ensemble allows a simultaneous relaxation of lattice and basis vectors obtaining a true ground state within the model. The computational efficiency of the method also makes calculational efforts for the 34 or 46 atom unit cells rather easy, allowing for the inclusion of an adequate number of  $k$  points to check for convergence in the force constants. In our calculations, we find 8  $k$  points in the full zone to be sufficient for obtaining converged results for phonons in both Clath34 and Clath46.

In Fig. 5 we show the phonon dispersion curves for Clath34 obtained using the GTBMD scheme using the method outlined in Ref. 24. Note that, in order to facilitate comparison with experiments, we have used a scale factor that normalizes the highest mode in the calculated diamond phase of Si to the experimental value. All the results for frequencies of clathrates reported in this work have been scaled by this factor. The spectrum for Clath34, while displaying the expected zone-folding effects, also contains

many interesting features. The most striking feature is the presence of a gap in the spectrum. This feature may be understood on general grounds by a consideration of the distribution of bond lengths in the unit cell. The presence of more than one bond length in the unit cell is effectively analogous to having more than one force constant, as is the case, for example, for hetero-atomic systems. Another interesting feature is the increase in frequency for the transverse optical ( $\Gamma_{TO}$ ) mode when compared to the diamond phase. This is perhaps not surprising when one considers the fact that even though the average bond length is larger than in diamond phase, one of the bond is shorter (2.343 Å). The largest frequency ( $\Gamma_{TO}$ ) obtained within the present scheme has a value of 528 cm<sup>-1</sup>. This mode is generated by a concerted motion of four nearest neighbors of a central atom towards it or away from it while the central atom remains stationary. Note that this mode is not present in the diamond phase of Si at zone center. This is a 2% increase that should be experimentally observable.

In Fig. 6 we show the phonon dispersion curves for Clath46 obtained using the present scheme. Once again, the spectrum, while displaying the expected zone-folding effects, also contains a gap in the spectrum. An interesting

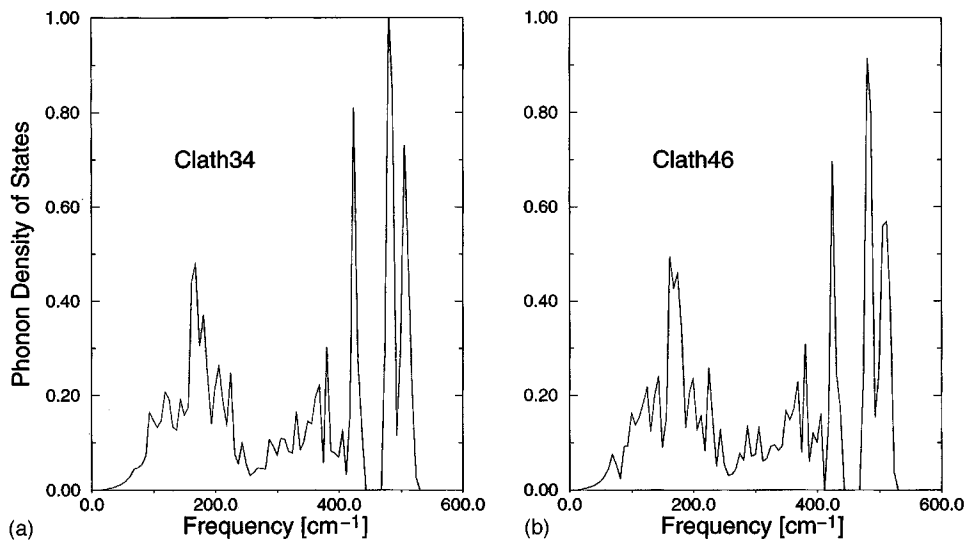


FIG. 7. Phonon density of states for (a) Clath34 and (b) Clath46.

TABLE II. Calculated vibrational frequencies at  $k=0$  for Clath34.

Symmetry	Frequency (cm <sup>-1</sup> )	Symmetry	Frequency (cm <sup>-1</sup> )
$A_{1g}^a$	305	$A_{1u}$	521
	395		
	498	$A_{2u}$	264
	383		
$A_{2g}$	178		431
$E_g^a$	124	$E_u$	154
	362		285
	481		485
	528		496
$F_{1g}$	124	$F_{1u}^b$	158
	141		176
	169		258
	423		376
	515		436
			482
			494
$F_{2g}^a$	157		
	260	$F_{2u}$	146
	307		158
	420		370
	479		482
	491		518
	518		

<sup>a</sup>Raman active.<sup>b</sup>Infrared active.

contrast, however, is the softening of the  $\Gamma_{TO}$  mode when compared to the diamond phase. Our value of 508 cm<sup>-1</sup> represents a 2% decrease when compared to the corresponding mode in the diamond phase. Additionally, the optical bands show even less dispersion when compared with Clath34 and the gap is narrower. This can be attributed to lesser dispersion in the bond lengths.

The phonon densities of states for both these clathrates are shown in Fig. 7.

### C. Theoretical Raman spectra

In this section we present theoretical results for intensities of the Raman-active modes using the eigenfrequencies and eigenvectors of the dynamical matrix used in obtaining the phonon spectra in Sec. III B. The bond polarizability model<sup>27,28</sup> is incorporated into the formalism to calculate the Raman spectra of these clathrates. The five fitting parameters for calculating the spectra (bond polarizabilities and their derivatives) were taken from Ref. 27 for Si.

The calculated Raman scattered intensity components  $I_{xx}$  and  $I_{xy}$  for Clath34 and Clath46 are shown in Figs. 8 and 9, respectively. Here,  $xyz$  are assumed aligned along the cubic crystallographic axes. Group theoretical analysis shows that the  $I_{xx}$  spectrum gets contributions from  $A_{1g}$  and  $E_g$  modes, while the  $I_{xy}$  spectrum gets contribution from  $F_{2g}$  modes.<sup>29</sup>

In Tables II and III we list the calculated vibrational frequencies at  $k=0$  for Clath34 and Clath46, respectively. As

TABLE III. Calculated vibrational frequencies at  $k=0$  for Clath46.

Symmetry	Frequency (cm <sup>-1</sup> )	Symmetry	Frequency (cm <sup>-1</sup> )
$A_{1g}^a$	328	$A_{1u}$	323
	431		483
	492		
		$A_{2u}$	140
$A_{2g}$	178		390
	226		
	388	$E_u$	159
	508		183
			479
			483
$E_g^a$	141		
	212		
	297	$F_{1u}^b$	136
	418		176
	471		196
489	289		
508	376		
			421
			474
$F_{1g}$	116		483
	139		493
	166		
	190		
	349	$F_{2u}$	132
	420		166
	484		232
	495		315
			371
$F_{2g}^a$	106		477
	170		485
	184		493
	291		
	415		
	477		
	485		
492			

<sup>a</sup>Raman active.<sup>b</sup>Infrared active.

before, our values for higher frequencies have been scaled down to facilitate comparison with experiment. Results shown in Tables II and III are in general agreement with the previous results of Alben *et al.*<sup>26</sup> obtained within a force constant model, although the details of the symmetry ordering are model dependent. The only experimental results for Raman scattering for Si clathrates are a study of  $M_x\text{Ba}_y\text{Si}_{46}$  ( $M = \text{Na}, \text{K}$ ) by Fang *et al.*<sup>12</sup> Clearly the cations are expected to affect the vibrational spectrum significantly, and a direct comparison is impossible. However, it is interesting to note that in  $\text{Na}_{0.2}\text{Ba}_{5.6}\text{Si}_{46}$  where Na concentration is fairly dilute, the most prominent features in the Raman spectrum are in the 500 cm<sup>-1</sup> and 350 cm<sup>-1</sup> range, qualitatively similar to our  $I_{xx}$  spectrum for the empty Clath46. As experimental methods of synthesis improve we can look for purer clathrate systems.

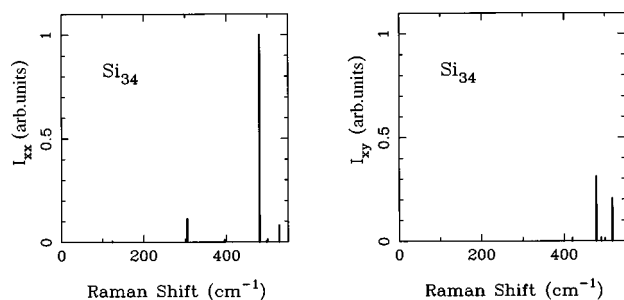


FIG. 8. Raman spectra for Clath34.

#### IV. SUMMARY

We have presented the results of our study of structural and vibrational properties of Si clathrates using a GTBMD scheme. The structures were optimized with GTBMD method incorporating constant pressure ensemble techniques which allowed for the full symmetry unrestricted relaxation of the lattice degrees of freedom. Both Clath34 and Clath46 are found to be highly stable with their energies only slightly higher than that of diamond Si. The relaxed structures show an increase in the volume per atom when compared to the bulk diamond phase and wide band gaps with values in the optical region. The relaxed structures also show a distribu-

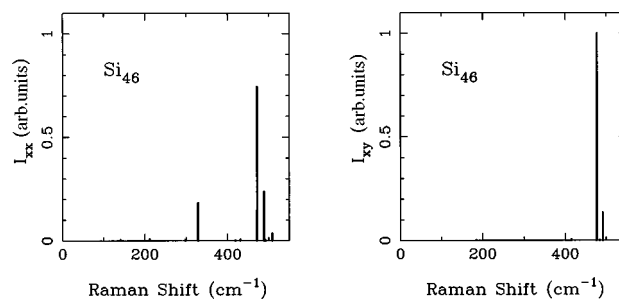


FIG. 9. Raman spectra for Clath46.

tion of bond lengths. The vibrational spectra of both clathrates contain gaps in the spectra. We have also presented the theoretical Raman spectra for these clathrates showing large peaks in the high frequency regions.

#### ACKNOWLEDGMENTS

We are grateful for useful discussions with O. F. Sankey and A. Demkov who also introduced us to this subject. We are also grateful to L. Grigorian for providing us with useful experimental information. This research was supported in part by U.S. DOE Contract No. DE-FC22-93PC93053, by NSF Grant No. OSR 94-52895, and by the University of Kentucky Center for Computational Sciences.

\*Electronic address: super250@convex.uky.edu

<sup>1</sup>L. T. Canham, Appl. Phys. Lett. **57**, 1046 (1990).

<sup>2</sup>A. G. Cullis and L. T. Canham, Nature (London) **353**, 335 (1991).

<sup>3</sup>F. Buda, J. Kohanoff, and M. Parrinello, Phys. Rev. Lett. **69**, 1272 (1992).

<sup>4</sup>M. S. Brandt, M. D. Fuchs, M. Stutzmann, J. Weber, and M. Cardona, Solid State Commun. **81**, 307 (1992).

<sup>5</sup>J. L. Mercer, Jr. and M. Y. Chou, Phys. Rev. B **49**, 8506 (1994).

<sup>6</sup>J. S. Kasper, P. Hagemuller, M. Pouchard, and C. Cross, Science **150**, 1713 (1965).

<sup>7</sup>G. B. Adams, M. O'Keeffe, A. A. Demkov, O. F. Sankey, and Y.-M. Huang, Phys. Rev. B **49**, 8048 (1994).

<sup>8</sup>A. A. Demkov, O. F. Sankey, K. E. Schmidt, G. B. Adams, and M. O'Keeffe, Phys. Rev. B **50**, 17 001 (1994).

<sup>9</sup>A. A. Demkov, W. Windl, and O. F. Sankey, Phys. Rev. B **53**, 11 288 (1996).

<sup>10</sup>E. Galvani, G. Onida, S. Serra, and G. Benedek, Phys. Rev. Lett. **77**, 3573 (1996).

<sup>11</sup>C. Cros, M. Pouchard, and P. Hagemuller, J. Solid State Chem. **2**, 570 (1970).

<sup>12</sup>S. Fang *et al.* (unpublished).

<sup>13</sup>M. Menon and K. R. Subbaswamy, Phys. Rev. B **47**, 12 754 (1993).

<sup>14</sup>M. Menon and K. R. Subbaswamy, Phys. Rev. B **50**, 11 577 (1994).

<sup>15</sup>M. Menon and K. R. Subbaswamy, Phys. Rev. B **55**, 9231 (1997).

<sup>16</sup>K. Raghavachari and C. M. Rohlfing, J. Phys. Chem **95**, 5768 (1991).

<sup>17</sup>M. Menon, E. Richter, and K. R. Subbaswamy, J. Chem. Phys. **104**, 5875 (1996).

<sup>18</sup>H. C. Andersen, J. Chem. Phys. **72**, 2384 (1980).

<sup>19</sup>M. Parrinello and A. Rahman, Phys. Rev. Lett. **45**, 1196 (1980).

<sup>20</sup>S. Nose, J. Chem. Phys. **81**, 511 (1984).

<sup>21</sup>W. G. Hoover, Phys. Rev. A **31**, 1695 (1985).

<sup>22</sup>A. Demkov, O. F. Sankey, and M. Menon (unpublished).

<sup>23</sup>In our scheme, the use of a minimal  $sp^3$  basis set leads to an overestimation of the band gap in the diamond structure. Any band gap estimations, therefore, must take into account a correction term that will bring the value of this gap in agreement with the experimental value of 1.17 eV.

<sup>24</sup>M. Menon, E. Richter, and K. R. Subbaswamy, J. Chem. Phys. **104**, 5875 (1996).

<sup>25</sup>G. Nilsson and G. Nelin, Phys. Rev. B **6**, 3777 (1972).

<sup>26</sup>R. Alben, D. Weaire, J. E. Smith, Jr., and M. H. Brodsky, Phys. Rev. B **11**, 2271 (1975).

<sup>27</sup>S. Go, H. Bilz, and M. Cardona, Phys. Rev. Lett. **34**, 580 (1975).

<sup>28</sup>D. W. Snoke and M. Cardona, Solid State Commun. **87**, 121 (1993).

<sup>29</sup>R. Loudon, Adv. Phys. **13**, 423 (1964).